Transport of Heavy Hydrocarbon and Its Redeposition on Plasma Facing Walls

Kaoru OHYA[1], Kensuke INAI[1], Yasuyuki KIKUHARA[1], Tomohide NAKANO[2], Jun KAWATA[3], Hayato KAWAZOME[4], Yoshio UEDA[4], Tetsuo TANABE[5]

[1]*The University of Tokushima, Tokushima 770-8506, Japan*

[2]*Japan Atomic Energy Agency, Ibaraki 311-0193, Japan*

3Takuma National College of Technology, Kagawa 769-1192,Japan

[4]*Osaka University, Osaka 565-0871, Japan*

[5]*Kyushu University, Fukuoka 812-8581, Japan*

(Received: 31 August 2008 / Accepted: 31 December 2008)

Redeposition of C_2H_4 and C_2H_6 chemically eroded from carbon walls is simulated by EDDY code incorporated by the reflection on a hydrogenated and amorphized carbon surface. The redeposition rate for heavy hydrocarbons is drastically decreased by introduction of the reflection. The redeposition patterns on the surface are enlarged by the reflection, but it is narrower for the heavy hydrocarbons than for CH_4. The photon emissions of C_2 from C_2H_4 (C_2H_6) decay faster than that of CH from CH_4 in high-temperature (>10 eV) plasmas, which reproduces the difference of the decay of the CD and C_2 light intensities observed in the vicinity of the outer diverter plates of JT-60U. For such temperatures, the calculated inverse photon-efficiency *D/XB* is in good agreement with the observed values, whereas it decreases faster with deceasing temperature up to 5 eV and then increases with a further decrease of temperature.

Keywords: plasma wall interaction, tritium inventory, hydrocarbon, redeposition, ethane, *D/XB*, JT-60U.

1. Introduction

In present fusion devices, plasma wall interaction of hydrogen isotope plasmas with carbon based walls leads to chemical erosion processes, resulting in hydrocarbon impurities. The hydrocarbon becomes redeposited on the surface which is a critical issue for safety operation with tritium. Transport of hydrocarbons, e.g. CH_4, released by chemical sputtering is of acute interest in an important mechanism. For low temperature (<10 eV) plasmas in a detached divertor, heavier hydrocarbons such as ethane (C_2H_y) and propane (C_3H_y) families becomes more important. We have conducted a computer simulation of redeposition characteristics of C_2H_4 and C_2H_6 and its comparison with those for CH_4. A common diagnostic method for the hydrocarbon influx from the wall is the analysis of radiation from the molecular fragments, where the correlation of CH and C_2 radiations with methane and ethane, respectively, are required as a so-called inverse photon-efficiency *D/XB*, being dependent on plasma parameters and hydrocarbon species. *D* describes the dissociation of the hydrocarbons into the fragments and *XB* denote the excitation rate coefficient *X* from ground state into the excited state times the branching ratio *B*. The *D/XB* values are used for the determination of hydrocarbon influx Γ_{CxHy} from the radiations Γ_{rad} of the fragments such as CH and C_2: $\Gamma_{CxHy}=(D/XB)\Gamma_{rad}$. Therefore, we have calculated the inverse photon-efficiencies *D/XB* from the ratios of the number of the launching CH_4, C_2H_4 and C_2H_6 molecules to the photon emission events of CH and C_2, and the plasma temperature dependence of the calculated CH and C_2 radiations is compared with the observed radiations of CD and C_2 in an outer divertor of JT-60U.

2. Simulation Models

For parameter studies, a simple model is used for simulation of hydrocarbon transport in a plasma with constant electron temperature and density; the ion temperature is assumed to be equal to the electron temperature. The rectangular volume above part of the surface with an area of 10 x 10 cm^2 is the simulation volume, where the thickness of the plasma is 10 cm. The angle of magnetic field lines with the toroidal direction is 5^o and the lines are inclined by 30^o against the poloidal direction; the magnetic field strength is 5 T. These values are relevant to the designed ITER divertor. 10^5 hydrocarbons with a thermal velocity distribution (0.1 eV) are launched from a position on the surface and their

author's e-mail: ohyal@ee.tokushima-u.ac.jp

complex dissociation/ionization reactions are followed using atomic data package from Janev/Reiter [1], according to the Monte Carlo scheme. In this study, for simplicity of CH and C_2 radiations from methane and ethane families in the plasma, the emission rate coefficients for the Swan band ($d^3\Pi_g$-$a^3\Pi_u$ transition with a band head at 516.5 nm for the vibrational band v'=v''=0) of C_2 and the Gerö band ($A^2\Delta$-$X^2\Pi$ transition with a band head at 431 nm, v'=v''=0-2) of CH, which were calculated with the IPProg code [2] are incorporated into our simulation of collisional reactions of hydrocarbons. When a particle produced by the reaction is charged, it gyrates perpendicular to the magnetic field lines and experiences friction and thermal gradient forces parallel to the lines, cross-field diffusion, sheath and presheath acceleration, as presented at elsewhere [3] with detailed discussion. In our simulation volume, constant plasma temperature is assumed; however, the thermal gradient force is important in that it competes with the friction force. Thus, for simplicity, the temperature gradient per meter was assumed to be equal to the plasma temperature. Each particle is pursued until it redeposits on the surface or escapes from the simulation volume.

The particles returning to the surface can stick (redeposit) or move back (reflect) into the plasma as different types of hydrocarbons. The surface reflection process is one of critical mechanisms for long-distance transport of carbons/hydrocarbons in the entire machine, although the other is re-erosion of the redeposited layers with rich hydrogens [4]. In this study, a classical molecular dynamics (MD) simulation is applied to evaluate the reflection coefficients of CH_4, C_2H_4 and C_2H_6, and all of the dissociation products on the surface. In MD, we use an interaction potential based on analytic bond-order scheme [5] and atomic trajectories in a temperature-controlled simulation cell are followed using a conventional technique; the detailed simulation models are presented in [6]. Hydrogenated and amorphized carbon surface is prepared as a starting surface by bombardment with 0.025 eV carbon and 1 eV hydrogen on crystalline tungsten. The calculated reflection coefficients of ethane and methane families are shown in Fig. 1(a) and 1(b), respectively. Due to the break-up of incident hydrocarbons, many different dissociation products are released from the surface, whereas in the figure, all species of CH_y and C_2H_y are taken into account. The dissociation due to the impact on the surface is more complex for C_2H_6 than for CH_4, in the same way as the collisional Reactions in the plasmas. With increasing energy and hydrogen content (i.e., y of CH_y and C_2H_y), the reflection coefficient decreases and increases, respectively, for both methane and ethane families due to

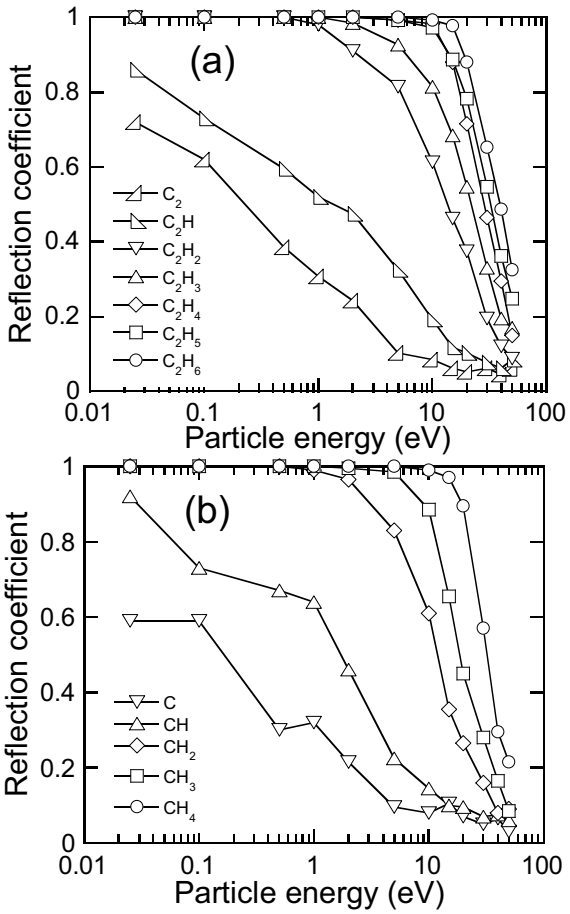

Fig. 1 Reflection coefficient for (a) C_2Hy (y=0-6) and (b) CHy (y=0-4) on a hydrogenated and amorphized carbon surface.

deeper penetration in the bulk and weaker attraction interactions with surface carbon atoms, respectively. Furthermore, heavy hydrocarbons (C_2H_y) are reflected more than CH_4. The trend can be explained by the interaction potential for each molecular configuration, which will be published in following paper with the comparison with experiments and other simulations.

3. Heavy Hydrocarbon Redeposition on Plasma Facing Wall*s*

For heavy hydrocarbons as well as methane, a much higher neutral fraction is redeposited at low plasma temperature due to a reaction chain of charge exchange with hydrogen ions and electron-impact dissociative recombination which produces many neutral fragments. At high plasma temperature, electron-impact ionization produces dominant ion fraction of redeposition species. In Fig. 2(a), both ion and neutral fractions are drastically decreased by introduction of the reflection (and dissociation) on the tile surface. This is because large molecules with large gyroradii and with high reaction rates decrease, which suppresses the local redeposition in

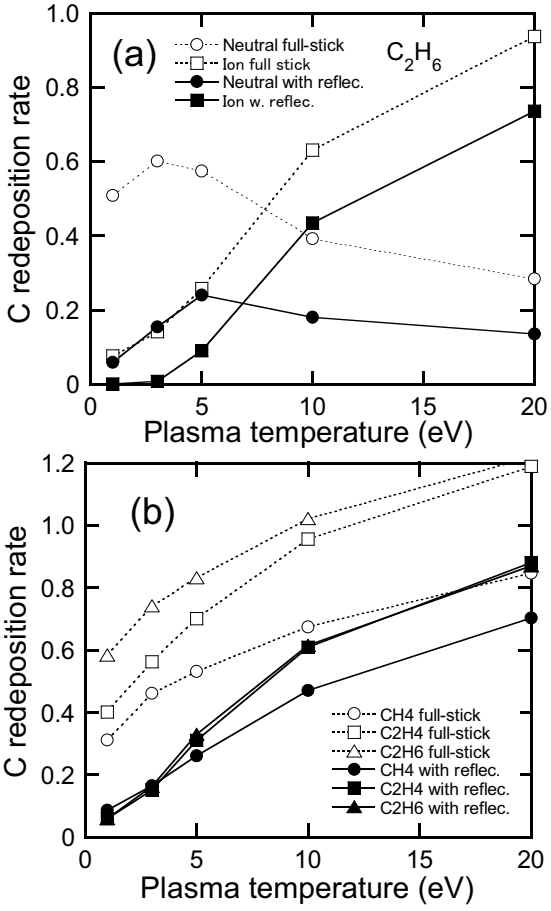

Fig. 2 (a) the C redeposition rate as ion species and neutral species per launched C_2H_6 and (b) total C redeposition rate per launched CH_4, C_2H_4 and C_2H_6 on the surface (10 x 10 cm^2) in terms of plasma temperature at plasma density of 10^{19} m^{-3}.

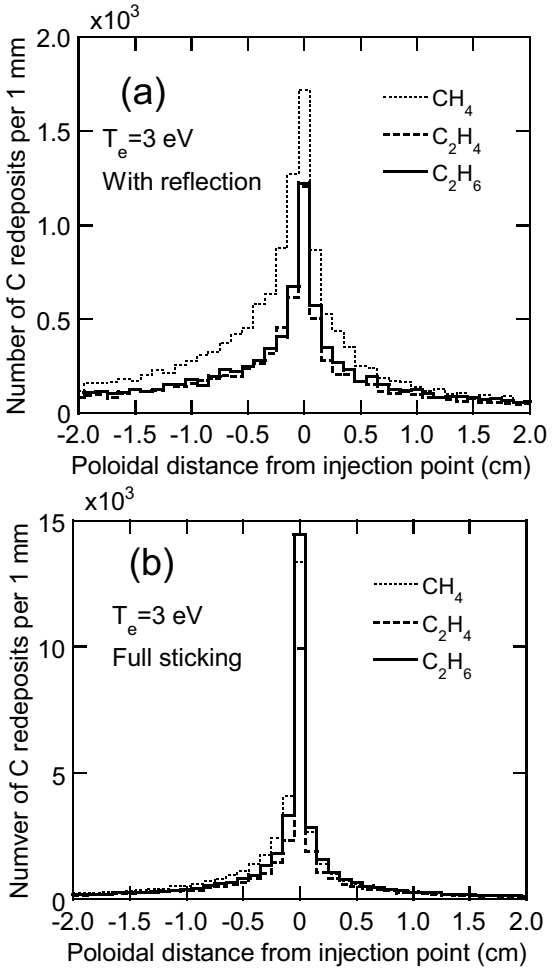

Fig. 3 Poloidal distributions of carbons/ hydrocarbons redeposited on the surface following the release of 10^5 CH_4, C_2H_4 and C_2H_6 at plasma temperature of 3 eV and plasma density of 10^{19} m^{-3}. In the case of (b), full-sticking of hydrocarbons returning the surface is assumed.

the vicinity of the released position. The C redeposition rate, in which the redeposition of C_2 are counted doubly, becomes larger for C_2H_6 and C_2H_4 with the large gyroradii than for CH_4 again, but the multiple reflection on the surface more efficiently suppresses the redeposition rate (Fig. 2(b)).

Redeposition patterns on the tile surface are largely dependent on the plasma temperature [7]. At low plasma temperature, the neutral species liberated from a magnetic constrain redeposit widely in both toroidal and poloidal directions. As shown in Fig. 3, such redeposition patterns distribute over the range of the order of cm at the plasma temperature of 3 eV and the density of 10^{19} m^{-3}. The patterns are enlarged due to the multiple reflection on the surface. In the cases of C_2H_4 and C_2H_6, the shape of patterns is similar to each other, but it is narrower than that for CH_4, probably due to higher reaction rates in the plasma and more frequent dissociation at the surface.

4. Molecular Radiation of Heavy Hydrocarbons in Divertor Plasmas

Figures 4(a) and 4(b) show the number decays of photon emission events of (a) CH from CH_4 and (b) C_2 from C_2H_6, respectively, in the plasma with different temperatures. The number of the photon emission events in the vicinity of the surface increases with decreasing temperature, but decreases at the temperature of 3 eV. The decrease is a result of a decreasing emission rate coefficient for both radiations. Due to fast progress of dissociation events and dominant ionization events, the decay length for both radiations shortens with increasing temperature. It should be noted that at high temperatures, the decay for C_2 is much shorter than for CH, whereas at low temperatures of the order of eV, they is similar to each other.

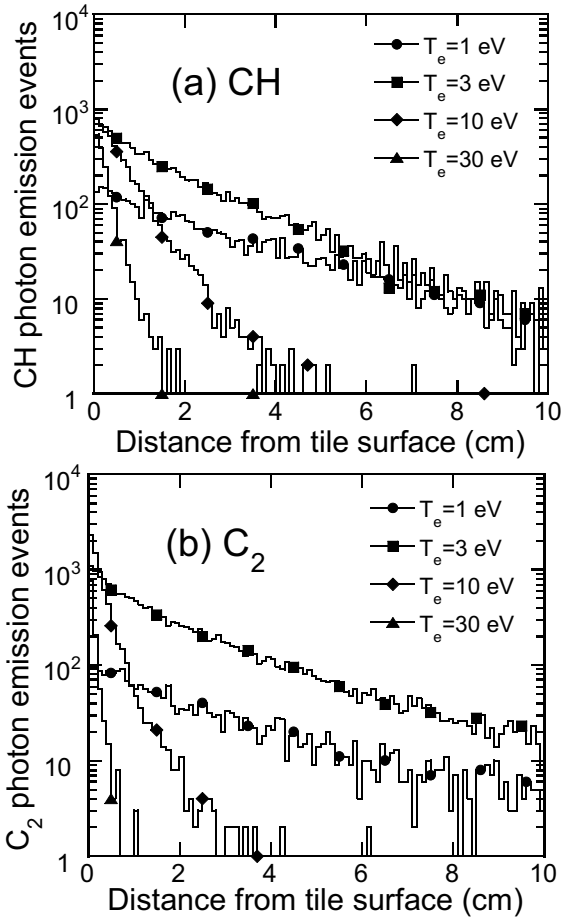

Fig. 4 Decay distribution of photon emission events of (a) CH from CH_4 and (b) C_2 from C_2H_6 in the plasmas with different temperatures. The constant plasma density is assumed to be 10^{19} m^{-3}.

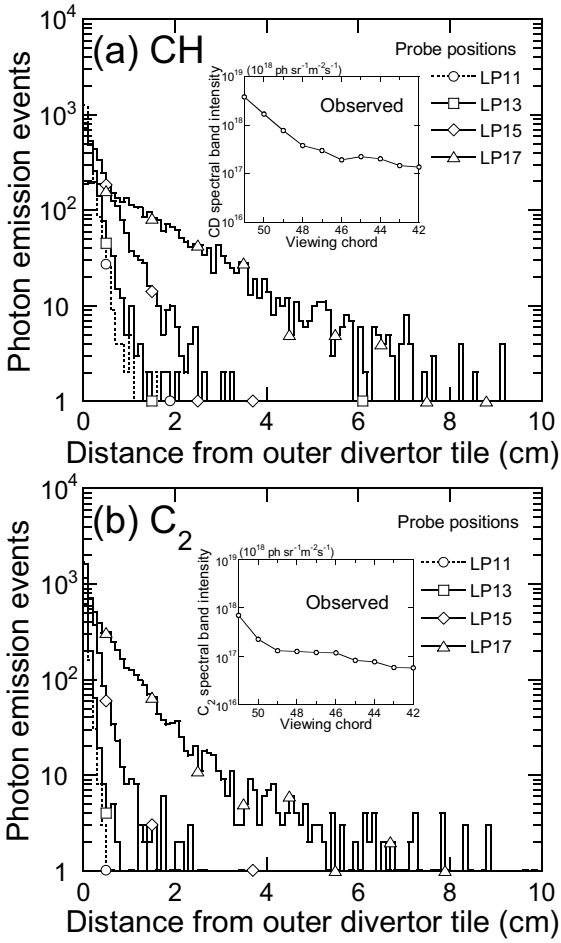

Fig. 5 Decay distribution of photon emission events of (a) CH from CH_4 and (b) C_2 from C_2H_4 in the vicinity of the outer divertor plates in JT-60U. The insets show the observed changes of CD and C_2 light intensities with the viewing chord near the plates.

For comparison of such calculations to the experimental observations, we performed further calculations with the plasma temperatures and densities measured using 9 Langmuir probes on the outer divertor plates in JT-60U [8]: the probes are called LP_{10}, LP_{11}, LP_{12}, LP_{13}, LP_{14}, LP_{15}, LP_{16}, LP_{17} and LP_{18} in the order from the bottom of the outer plates, and the probe LP_{11} is placed near the strike point. Details of the experiments and conditions were described in [8]. The plasma temperature and density used for simulation are 24 eV and $2x10^{19}$ m^{-3}, respectively, at the position of the probe LP_{11}, whereas they are 11 eV and $1.6x10^{18}$ m^{-3}, respectively, at the position of the probe LP_{18} which is 26 cm apart from the strike point. In this calculation, the angle of magnetic field lines with the toroidal direction is taken to be 2^o and the lines are inclined by 20^o against the poloidal direction; the magnetic field strength is 2.7 T. The calculated distributions of CH and C_2 photon emissions from CH_4 and C_2H_4, respectively, launched from four positions of the probes are shown in Fig. 5.

Although the decay length of the calculated distributions for both CH and C_2 strongly depends on the position on the outer divertor plates, all of the distributions show that the C_2 radiations decay faster than the CH radiations. This result reproduces the difference of the observed light intensities between CD and C_2, as shown in the insets of Fig. 5(a) and 5(b), respectively. Furthermore, the CH photon emission from C_2H_4 (also C_2H_6) shows similar decay to that from CH_4. Since the observed distributions correspond to the sum of the line of sight along each viewing chord, the calculated distributions at each position are summed after weighted by the incident ion fluxes, assuming the same erosion rates of CH_4 and C_2H_4 at all positions of the probes. The calculated distributions for both CH and C_2 decay somewhat faster than that of the observations. The reason for the deviation is not clear now, but some possibilities, e.g. position-dependent (or surface temperature-dependent) erosion rates of

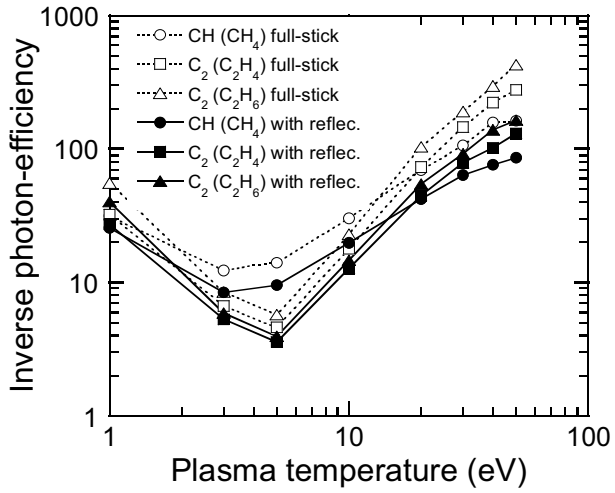

Fig. 6 Inverse photon-efficiency, *D/XB*, for CH from CH_4 and C_2 from C_2H_4 and C_2H_6. The constant plasma density is assumed to be 10^{19} m^{-3}.

hydrocarbons and geometry of the viewing chord and the tile arrangement, can be considered.

The inverse photon-efficiency *D/XB*, which relates the flux of eroded hydrocarbons to the emitted CD (also C_2) light intensity, is a critical factor in the study of chemical sputtering by spectroscopic measurements. Our simulation can estimate such factors which are defined as the ratio of the number of the launching hydrocarbons to the number of photon emission events for CH and C_2. Figure 6 shows the temperature dependence of *D/XB* for CH from CH_4, and C_2 from C_2H_4 and C_2H_6 in the conditions of the full-sticking and the multiple reflection at the tile surface. The *D/XB* efficiency decreases with decreasing temperature up to 5 eV and then increases with a further decrease of temperature due to a decreasing rate coefficient for CH and C_2 radiations. This dependence is similar to that with the ERO calculation for CD [9]. Furthermore, the efficiency for high plasma temperatures, e.g. 50 eV, is in reasonable agreement with the experimentally determined values [10]: ~100 for CH from CH_4 and ~550 for C_2 from C_2H_6. However, the calculated efficiency at low plasma temperatures of less than 10 eV tends to underestimate the observations. The observed *D/XB* values for CH (CD) from CH_4 (CD_4) show much slower decrease with decreasing plasma temperature and the increase at the temperatures of less than 5 eV are not found. Furthermore, by introduction of the multiple reflection on the surface, the *D/XB* values decreases due to additional photon emissions of the reflected CH and C_2.

5. Concluding Remarks

Transport simulation of C_2H_4 and C_2H_6, as well as CH_4, in plasmas were performed using a Monte Carlo collision simulation, where the reflection on the tile surface was taken into account. Both ion and neutral fractions of redeposition were drastically decreased by introduction of the reflection on the surface. The reflection more efficiently suppressed the redeposition rate of C_2H_4 and C_2H_6 than for CH_4. The redeposition patterns on the surface were enlarged due to the multiple reflection, but it is narrower for C_2H_4 and C_2H_6 than for CH_4. Furthermore, the photon emissions of CH from CH_4 and C_2 from C_2H_4 and C_2H_6 in the plasma were simulated for the basis of a correlation of measured molecular radiations with chemical sputtering of carbon walls in fusion devices. The C_2 photon emission decayed faster than that of CH, which reproduced the difference of the decays of CD and C_2 light intensities observed in the vicinity of the outer diverter plates of JT-60U, but the calculated decay for both CH and C_2, assuming the same erosion rates of CH_4 and C_2H_4 everywhere, was faster than the observed ones. At high plasma temperatures of the order of tens of eV, the inverse photon efficiency *D/XB* was in reasonable agreement with the values observed in JT-60U experiments, whereas the calculated values decreased with deceasing temperature up to 5 eV and then increases with a further decrease of temperature. The precise determination of the *D/XB* values for CH_4 (CD_4) and heavier hydrocarbons is of acute importance to estimate the chemical sputtering yield of carbon components from spectroscopic measurements in the divertor regions of ITER, in particular for low-temperature (<10eV) plasmas. Therefore, the validation of the simulation models including atomic data in plasmas and on surface are being continued presently by further comparison between the simulated and experimental results.

Acknowledgement

This work was supported by KAKENHI (190055005).

References

[1] R.K. Janev, D. Reiter, Rep. Forschungszentrum Jülich, Jül-3966(2002)/ Jül-4005(2003).
[2] U. Fantz et al., J. Nucl. Mater., 337-339, 1087(2005).
[3] K. Inai, K. Ohya, Jpn. J. Appl. Phys. 46, 1149(2007).
[4] T. Tanabe, Fusion Eng. Des. 81, 139(2006).
[5] N. Juslin et al., J. Appl. Phys. 98, 123520(2005).
[6] K. Inai, Y. Kikuhara, K. Ohya, Surf. Coat. Technol., 202, 5374(2008).
[7] K. Ohya, T. Tanabe, J. Kawata, Fusion Eng. Des. 81, 205(2006).

[8] T. Nakano et al., J. Nucl. Mater. 363-365, 1315(2007).
[9] A. Kirschner et al., J. Nucl. Mater. 313-316, 444(2003).
[10] T. Nakano et al., ITPA D/SOL Meeting, Univ.of Toronto, Canada, Nov. 6-7, 2006.